Biochimica et Biophysica Acta 1838 (2014) 902–909

Contents lists available at ScienceDirect

Biochimica et Biophysica Acta

journal homepage: www.elsevier.com/locate/bbamem

Numerical study of lipid translocation driven by nanoporation due to multiple high-intensity, ultrashort electrical pulses

Viswanadham Sridhara [a], Ravindra P. Joshi [b,*]

[a] Center for Computational Biology and Bioinformatics, College of Natural Sciences, University of Texas, 2415 Speedway, C4500, Austin, TX 78712, USA
[b] Dept. of Electrical & Computer Engineering, Frank Reidy Center for Bio-Electrics, Old Dominion University, Norfolk, VA 23529-0246, USA

ARTICLE INFO

Article history:
Received 28 June 2013
Received in revised form 1 November 2013
Accepted 5 November 2013
Available online 13 November 2013

Keywords:
Nanopore
Translocation
Lipid
Molecular Dynamics
Electric pulsing

ABSTRACT

The dynamical translocation of lipids from one leaflet to another due to membrane permeabilization driven by nanosecond, high-intensity (>100 kV/cm) electrical pulses has been probed. Our simulations show that lipid molecules can translocate by diffusion through water-filled nanopores which form following high voltage application. Our focus is on multiple pulsing, and such simulations are relevant to gauge the time duration over which nanopores might remain open, and facilitate continued lipid translocations and membrane transport. Our results are indicative of a $N^{½}$ scaling with pulse number for the pore radius. These results bode well for the use of pulse trains in biomedical applications, not only due to cumulative behaviors and in reducing electric intensities and pulsing hardware, but also due to the possibility of long-lived thermo-electric physics near the membrane, and the possibility for pore coalescence.

1. Introduction

The cells of all life forms are surrounded by a membrane, consisting of lipids, proteins, and small solutes solvated in the cellular fluid. This serves as a hub in mediating numerous cellular functions. One of the important membrane functions is that of transporting polar or non-polar molecules across the cell, and/or the re-organization and re-structuring of membrane molecules [1]. In particular, ion transport is of significant interest, since cell membranes strive to maintain the ionic electrochemical gradient, which is important for a variety of activities, such as ATP synthesis, transport of nutrients, and conveyance of electrical signals.

The other type of biologically relevant molecular trafficking is the translocation of lipid molecules across membranes (i.e., the lipid flip-flops). In general, plasma membranes are asymmetric with regards to the distribution of lipids across their membrane [2,3]. For example, the phosphatidylserine lipids are normally localized in the inner leaflet of plasma membranes, and their externalization is associated with cells undergoing programmed cell death and aids in the recognition and clearing of these cells from the healthy tissues of the organism [4,5]. This asymmetry is crucial for an array of cellular functions and plays an important role, for example, in membrane mechanical stability [6] and the modulation of the activity of membrane proteins [7]. Failure to maintain the asymmetric distribution of lipids can have dramatic and deleterious consequences.

Conventionally, lipid movements (i.e., passive flip-flops) are thermally induced and are very slow due to an unfavorable energy barrier of about 20–50 kcal/mol associated with the translocation of the polar head group through the low dielectric permittivity hydrocarbon core of the bilayer. Consequently, the rate of passive flip-flops of phospholipids is extremely small, on the order of 10^{-5} s^{-1} [8], i.e., on average, a single lipid experiences a thermally induced flip-flop every 24 h. The asymmetric transmembrane lipid distribution in living cells is maintained through active mechanisms that selectively transport lipids across a membrane using specialized proteins called flippases [9,10]. For example, the plasma membrane is marked by a strong asymmetry in its lipid composition, with phosphatidylcholine and sphingomyelin predominantly present in the exoplasmic leaflet, while phosphatidylserine and phosphatidylethanolamine are clustered around the cytosolic leaflet [11].

However, the structure of the cell membrane, which is primarily a lipid bilayer in the liquid-crystal phase, can be altered and reorganized by a host of external means [12]. In particular, a stable water-filled pore structure penetrating the membrane can be created that increase the cell permeability, and thus be used for noninvasive molecular delivery into cells [13,14]. Other applications of cell permeabilization brought about by membrane re-structuring, include introduction of genes [15,16], cell fusion [17], electrochemotherapy for cancer treatment [18], and transdermal delivery of drugs and genes. Though stimuli based on external voltages (leading to electroporation [19]), or ultrasonic pressure (leading to sonoporation [20]) have been common methods for pore formation, cell membrane characteristics can be altered by a variety of other means as well. These include laser triggers

Abbreviations: MD, Molecular Dynamics; PS, phosphatidylserine; DPPC, dipalmitoylphosphatidylcholine; ATP, adenosine triphosphate; TMP, transmembrane potential

* Corresponding author.
E-mail address: rjoshi@odu.edu (R.P. Joshi).

0005-2736/$ – see front matter © 2013 Elsevier B.V. All rights reserved.
http://dx.doi.org/10.1016/j.bbamem.2013.11.003

[21–24], biochemical analytes [25–27], changes in pH [28–30], temperature variations [31], and by pore forming toxins [32].

Experimental data indicates that passive lipid translocation across a membrane is a pore-mediated process [33]. Furthermore, electric pulses leading to electroporation have been shown to enhance the transbilayer mobility of phospholipids [34]. In the context of the nanosecond duration, high electric-pulses, it was shown several years ago through Molecular Dynamics (MD) simulations [35], that the formation of nanopore defect formation can lead to phosphatidylserine (PS) externalization in membranes over times scales on the order of ~10 ns. This process was shown to preferentially begin on the anode side, and that it was a nanopore facilitated event, rather than the result of molecular translocation across the trans-membrane energy barrier. Transport of the anionic PS headgroups was shown to commence even while pore formation in response to a ultrafast external electric pulse was still ongoing [36]. These reports collectively suggest that a major fraction of passive lipid translocations can take place through water defects (or pores) if they happen to be formed in membranes — whether artificially or naturally.

The use of high intensity (with electric fields at or above 100 kV/cm), short-duration (~10–100 ns range) pulses have recently been investigated for a range of biomedical applications [37,38]. Apart from electroporation (which should then also facilitate lipid flip-flops), reported effects include electrically-triggered intra-cellular calcium release [39,40], shrinkage of tumors [41], cellular apoptosis [42], temporary blockage of action potential in nerves [43], and activation of platelets for accelerated wound healing [44]. However, the aspect of lipid translocation has not been well studied or analyzed. Since lipid asymmetry is a ubiquitous property of the plasma membrane bilayer and its maintenance and loss play important roles in cell physiology (such as blood coagulation and apoptosis), it becomes germane to analyze this lipid translocation aspect in the context of electrically stimulated cell responses.

Here, in this contribution, we focus on lipid translocation from one leaflet to another due to membrane permeabilization driven specifically by nanosecond, high-intensity (>100 kV/cm) electrical pulsing of biological cells. Previous reports on electroporation have tended to focus primarily on the pore creation process. Here, we show that lipid molecules can translocate by diffusion via the water-filled nanopores. An additional aim is to probe the pore dynamics over longer time scales. Such simulations over longer times would be relevant to: (i) gauge the time duration over which the nanopores can remain open, and thus facilitate continued lipid translocations, and (ii) to study the extent to which multiple pulsing could have strong cumulative effects on cell response and membrane transport. Though experimental biomedical applications have always relied on using pulse trains, a theoretical explanation is lacking and it is not clear whether some optimal point may exist. Perhaps the requisite electric field intensities and the total external energy input for achieving desired bio-effects and the pulsing hardware could be reduced or optimized to advantage.

2. Methods and methods

The dynamics of pore formation, water entry and subsequent lipid translocation is studied here on the basis of Molecular Dynamics (MD) simulations performed using GROMACS [45] with a 2 fs time step. Typically, MD simulations in such situations are carried out by selecting a segment of the lipid bilayer membrane and constructing initial geometric arrangement of all the atoms and their bonding angles. Here dipalmitoylphosphatidylcholine (DPPC) lipids were used for the membrane. Regions of water are then defined on either side of the membrane to form the total simulation space. The force field parameters were taken from the united atom field of Berger et al. [46]. Simulations were at constant particle number and temperature (300 K), using a Berendsen thermostat [47] with a time constant of 0.1 ps for DPPC and water. Semi-isotropic weak pressure coupling (compressibility 4.5×10^{-5} bar^{-1}, time constant 1 ps) was employed with pressure set to 1 bar. Long-range electrostatic interactions were computed with a particle mesh Ewald method [48] with a cutoff radius of 1 nm, a grid width of 0.15 nm, and periodic boundary conditions. A 0.9/1.2 nm group based twin cutoff scheme was employed for the Lennard–Jones interactions. The linear constraint solver (LINCS order 4) algorithm outlined by Hess et al. [49] was used to constrain all the bond lengths within the lipids and on the water geometry. As is well known, the MD technique for any given simulation scenario can yield results that depend on the initial values assigned, specifically the molecular velocities. Here for statistical significance, a total of six MD simulations were carried out with different starting molecular velocities for the various conditions simulated and discussed in the next section. All simulations were performed using the GROMACS suite [50]. The trends were generally consistent, and the results shown in the next section represent typical simulation outcomes.

3. Results

One of the important aspects of electric-pulsing of biological cells relates to the differences (and potential efficiency) between multiple pulses versus single pulsing. Experimental reports in the literature [51] indicate that a train of 100 pulses requires 3–5 times less electric field intensities to produce the same increase in membrane conductance (a typical bio-effect) as compared to a single pulse. Also notably, multiple pulses lowered the threshold electric-field intensity from ~6 kV/cm for a single pulse to ~1.7 kV/cm for 100 pulses in GH3 rat cells [51]. This is certainly an important practical consideration for reducing the complexity and the voltage requirements of the hardware and electrical pulsing systems for biomedical applications. Similar advantage in using multiple pulse electroporation for the uptake of macromolecules by individual cells had been reported as early as 1992 by Weaver et al. [52]. A more recent report suggests that the bioelectric effects caused by ultrashort pulses scale with the square root of the pulse number [53]. This square root dependence on the pulse number points to a statistical motion of cells between pulses with respect to the applied electric field, and was explained using an extension of the random walk statistical results to random rotations. More importantly, though, the cumulative bio-effects of multiple pulsing suggest negligible membrane repair between successive nanosecond pulses. This conclusion is also in line with the observation of long-lived enhancements in membrane conductance following nanosecond, high-intensity pulsing [54].

To study the above point, Molecular Dynamics (MD) simulations were carried out to probe poration dynamics in response to external electric pulses. Since MD simulations are very computer intensive and require very small time steps (e.g., 2 fs used here), we chose to follow membrane dynamics over 2 pulses spanning a 70 ns interval. The time-dependent MD simulated the response of a membrane patch to two 10 ns rectangular pulses, separated by a 50 ns OFF interval. The electric field for each pulse was taken to be at a constant value of 0.6 V/nm; though high it is in the range used in many MD simulations. The transmembrane potential (TMP), however, will not remotely approach such high fields, since poration would set in prior to such a situation; leading to an effective shorting of the membrane conductivity. Practical TMP values for nanosecond pulsing have been reported to be around 1.6 V [55]. As shown theoretically by the Weaver group [56], large TMP values lead to logarithmic reductions in poration times. For each simulation run, the system was initially equilibrated with no field applied for the first 5 ns after the energy minimization step. The central goal was to study the poration dynamics and ascertain whether the pore, if formed, could remain open well after the electric field had ceased. In addition, any possible cumulative effects of the dual pulse, in terms of the pore opening and potential for continued expansion, were also probed.

In our MD simulations, the water–membrane system contained 37,157 water molecules and 512 dipalmitoylphosphatidylcholine (DPPC) lipid molecules for a total of 137,071 atoms in a 12.948 nm × 12.999 nm × 10.364 nm simulation box. This membrane

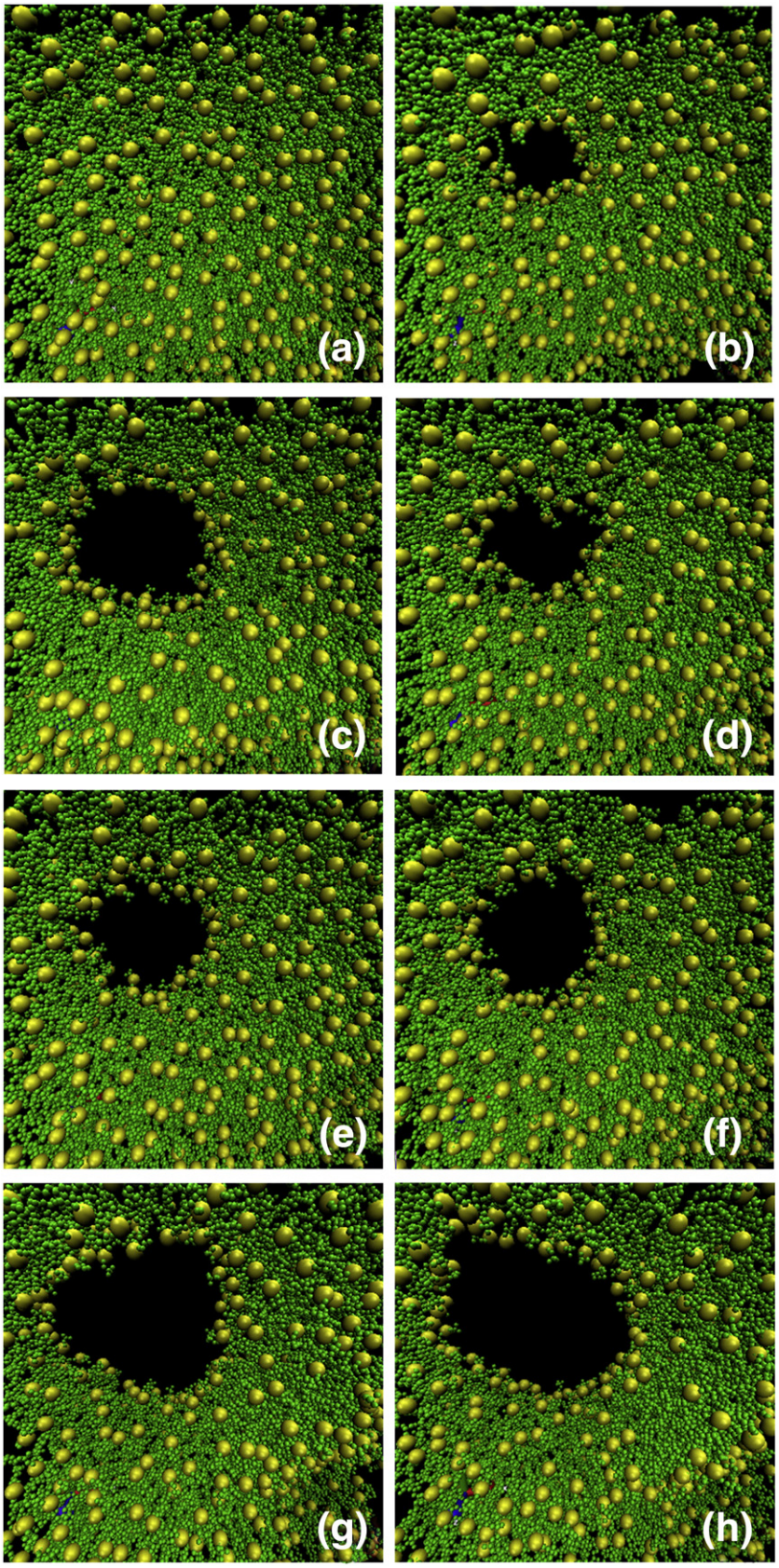

Fig. 1. MD results showing poration process in a DPPC membrane in response to two 10 ns rectangular pulses, separated by a 50 ns OFF interval. The electric field for each pulse was taken to be at a constant value of 0.6 V/nm. The yellow spheres represent the lipid headgroups, and the green wires denote the phospholipid tails. (a) Initial bilayer membrane with 37,157 water and 512 DPPC lipid molecules in a 12.948 nm × 12.999 nm × 10.364 nm simulation box. (b) Snapshot at 5 ns showing a pore beginning to form. (c) The t = 10 ns snapshot at the end of the first pulse showing a much bigger pore. (d) Situation after 15 ns after the end of the pulse showing only a slight reduction in pore size. (e) A t = 20 ns snapshot that reveals a mostly stable pore even in the absence of an external electric field. (f) The t = 60 ns snapshot at the beginning of the second electric pulse. (g) A 65 ns snapshot showing an expansion in the pore, and (h) The biggest pore size at the end of the second 10-ns electric pulse, 70 ns from the initial start of the simulations.

system was charge neutral, and represents a homogeneous section of a simple membrane as a test case of the lipidic system. Fig. 1(a)–(g) shows the MD results, and reveals a gradual pore creation that begins during the ON-time of the first pulse over the initial 10 ns regime. Fig. 1(a) is the starting snapshot at t = 0 instant of the unruptured membrane patch. The next t = 5 ns snapshot shown in Fig. 1(b), reveals the existence of a small nanopore; and this then is seen to grow bigger by the 10 ns time instant as apparent from Fig. 1(c). Upon termination of the electric pulse at 10 ns and up to 60 ns, the pore is seen to remain without undergoing significant changes or shrinkage. Fig. 1(d) which is a 15 ns snapshot, and Fig. 1(e) which is a 20 ns snapshot, are both fairly similar, and reveal a net pore size that remains roughly comparable to that of Fig. 1(c). These results clearly demonstrate that in the absence of an external driving electric-field, the pore once formed in the lipid membrane, does not tend to quickly collapse and shrink. The 60 ns snapshot of Fig. 1(f) shows nearly the same size. In addition, the plots show that the pore is not exactly circular as is routinely assumed in macroscopic, continuum analyses [38,57–60], and that there are constant and continuous random fluctuations in shape and size. Finally, upon the commencement of the second 10-ns pulse, the results show that the pore begins to get bigger. The 65 ns snapshot shown in Fig. 1(g), reveals the pore size to have increased. At the very end of the 2-pulse train, the pore in Fig. 1(h) is seen to be at its biggest. Thus overall, a cumulative effect is predicted for pore growth, and that the two-pulse wave train produces a bigger pore that has an area almost twice that from a single 10-ns pulse.

A clearer view of the membrane dynamics and time-dependent evolution of the pore size due to the two-pulse train is shown in Fig. 2. Upon pulse application, the pore is predicted to have a strong growth at a fairly constant rate during the first 10 ns of the pulse ON-time. A pore radius of about 2.2 nm was obtained from the simulations. Upon pulse termination at 10 ns, a slight decrease in size is predicted, and the pore radius is seen to settle around a 1.75 nm level, though with continuous fluctuations. This demonstrates that pore closure is a slow process, and at least over the nanosecond time scales following pulse termination, the membrane does not heal itself completely or recover to its initial unporated state.

Next, we examined the likelihood of pore-based lipid transport between the two membrane leaflets. Any such movement would naturally work to reduce existing asymmetries in the spatial distributions, and as such drive the cells further out of equilibrium. This asymmetry is crucial for an array of cellular functions and plays an important role in membrane mechanical stability and activity of membrane proteins. Fig. 3 shows a series of snapshots obtained from the MD simulations in response to the two-pulse excitation spanning a total of 70 ns. In the figure, the yellow and red spheres denote the lipid headgroups at the top and bottom membrane surfaces, while the green strings shown in the pictures represents two specific lipid molecules. The water molecules are shown in purple color. Fig. 3(a) shows the initial bilayer membrane with most of the lipids shown as thin films for clarity. Two specific lipids were tracked. Both are denoted in green and occur at the top and bottom sides of the DPPC membrane. The next figure (Fig. 3b), which is a snapshot at 5 ns, shows pore formation and lipid movements within the pore. The t = 10 ns snapshot shown in Fig. 3(c) is at the end of the first pulse, and clearly shows some more lipid inter-mingling (as seen from the yellow and red spheres) and the expansion of the pore. The 15 ns simulation result after the end of the pulse shown in Fig. 3(d), reveals the slow downward descent of the chosen green lipid at the upper leaflet, while the pore roughly remains intact. The other chosen lipid on the bottom leaflet is masked and not seen very clearly. Fig. 3(e) is a t = 20 ns snapshot in the absence of an external electric field. The t = 60 ns picture at the beginning of the second electric pulse is shown in Fig. 3(f). This view shows the upward movement of the second chosen lipid that was initially at the bottom leaflet. At 65 ns, the pore is seen to be wider in Fig. 3(g), more of the yellow and red lipids have changed positions, and the marked green lipid strings have moved further to the opposite leaflets. Finally, at the end of the second 10-ns electric pulse, 70 ns from the initial start of the simulations, Fig. 3(h) shows the nearly complete translocation of the green-lipidic string to the bottom on the left, and the near-compete upward movement of the second string to the top. It may also be mentioned that overall six lipids actually translocated, though only 2 were shown highlighted for simplicity in Fig. 3. Not only do these results demonstrate pore-mediated lipidic movement, but also reveal that the second pulse actually takes the lipid faster to the other side than the first one. This is not surprising if one accepts that the lipid translocation is a pore-mediated event. The pore has more water molecules and is also wider during the second pulse, indicating that the local environment is much less hydrophobic and the energy barrier (or space constriction) associated with lipidic repulsions has reduced. As a final point, it may be mentioned that we deliberately chose to simulate a zwitterionic lipid (DPPC) rather than focus on a charged entity such as phosphatidylserine (PS). A charged molecule (such as PS) would be acted upon by an electrostatic force in the presence of an externally applied electric field. It would thus be somewhat easier for a charged PS molecule to translocate when subjected to the influences of an external electric field. Thus here in a sense, we take the "worst case scenario" of an uncharged lipid molecules, and show that due to the underlying poration process, even such molecules can be translocated. However, PS and other molecules distributed asymmetrically too, would be able to move based on diffusion through the nanopores.

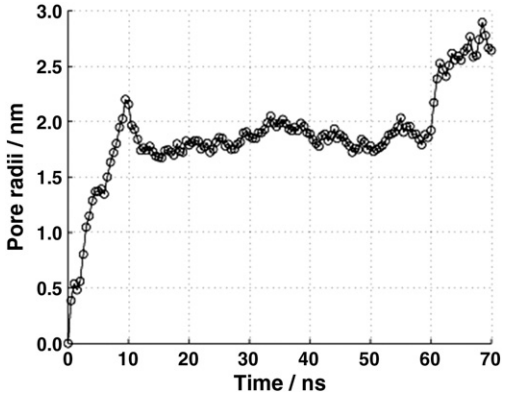

Fig. 2. MD result showing the temporal evolution of the pore radius in response to the two-pulse excitation.

4. Discussion

The relatively long-lived nature of the electropore and its subsequent expansion upon application of the second electric pulse is first discussed. A plausible consequence of multiple pulsing could be the formation of fairly large nanopores. In the results of Fig. 2, for example, the pore radius has been predicted to grow from ~1.75 nm after the first pulse to about 2.51 nm following the second pulse. This growth in pore radius is sub-linear with the radius roughly scaling by 1.43, and thus the ratio of the areas increases by a factor of 2. Though our simulation data is by no means extensive, these ratios do seem to point out two very interesting features: (i) The scaling effect on the pore radius roughly tends to $N^{½}$, a prediction that had previously been reported purely based on statistical arguments [53]. Hence, by increasing the number of pulses, one might get a distribution of much bigger pores on the plasma membrane. (ii) The total pore area does indeed double, and so one can expect many more entry-sites for the possible transport of big molecules and drugs from the external medium into cells. This could be very beneficial from the standpoint of electro-chemotherapy, for which the principle goal is to enhance the permeability of specific large-sized drugs (e.g., Bleomycin) into tumor cells. Since some of the drug molecules can be large-sized (e.g., over 4 kDa), the availability of larger-sized

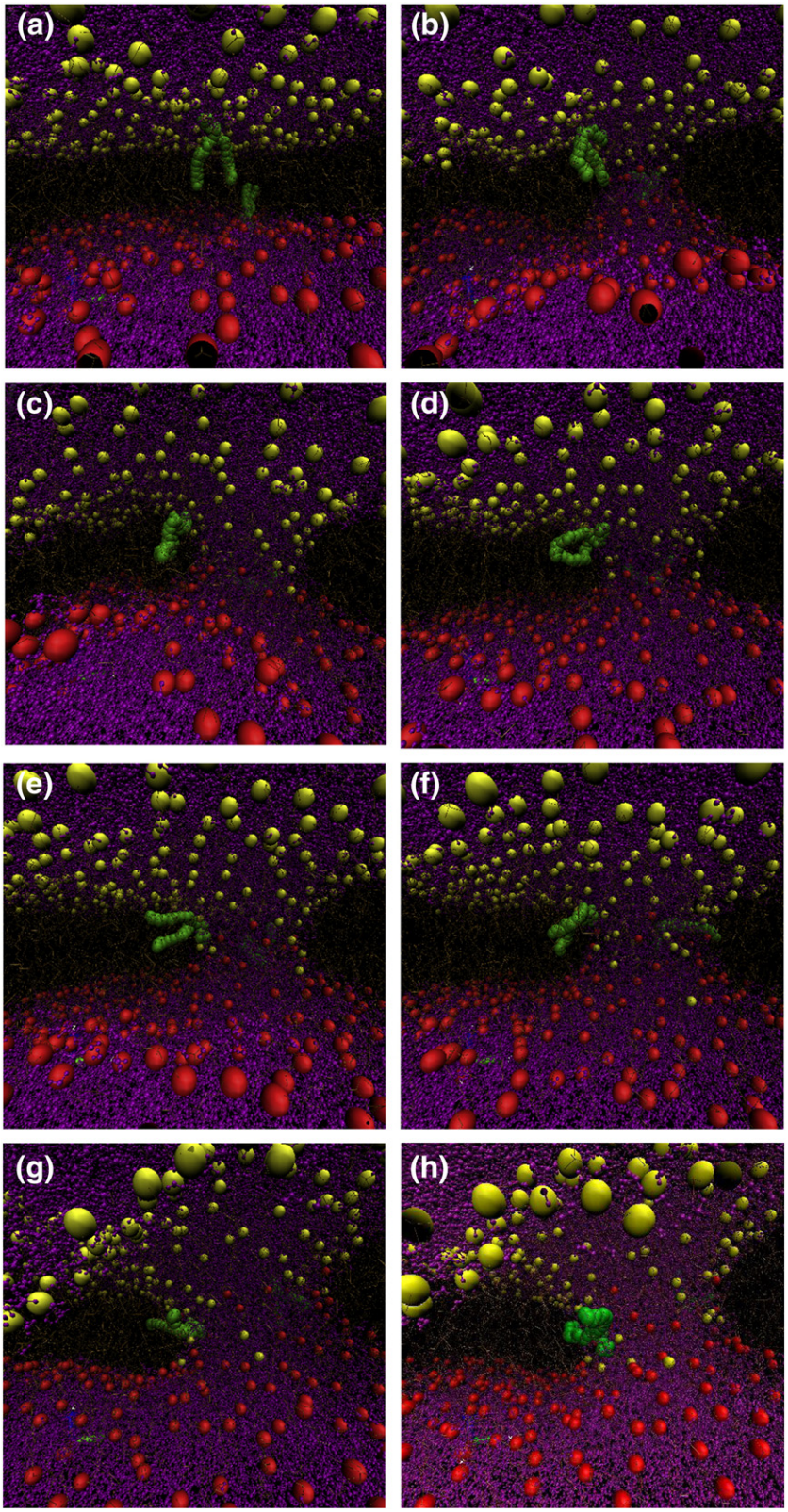

Fig. 3. MD results showing pore-mediated lipid translocation for the conditions of Fig. 1 involving two 10 ns rectangular pulses, separated by a 50 ns OFF interval. The yellow and red spheres denote the lipid headgroups at the top and bottom membrane surfaces, while the green strings represent two specific lipid molecules. The water molecules are shown in purple color. (a) Initial bilayer membrane denoting the intact membrane. (b) Snapshot at 5 ns showing pore formation and lipid movements within the pore. (c) The t = 10 ns snapshot at the end of the first pulse showing a slightly greater lipid movement. (d) Situation at 15 ns after the end of the pulse showing the slow downward descent of the chosen green lipid. (e) At t = 20 ns snapshot in the absence of an external electric field. (f) The t = 60 ns picture at the beginning of the second electric pulse. (g) At 65 ns (i.e., 5 ns after the start of the second pulse), the pore is wider, more of the yellow and red lipids have changed positions, and the marked green lipid has descended further. (h) At the end of the second 10-ns electric pulse, 70 ns from the initial start of the simulations, showing the nearly complete translocation of the green-lipidic string, with further intermingling of the yellow-and-red lipids.

pores would certainly facilitate and enhance the desired molecular throughput. On a related note, it may also be mentioned that it is very likely that use of multiple pulsing (along with higher applied voltages), could lead to a higher pore density. Such a higher pore density would be very conducive to pore coalescence and once again, promote the emergence of larger sized entry sites at the plasma membrane.

The scaling argument is somewhat tenuous not only because results here are available from only 2 pulses, but also because the results would depend on the ongoing dynamics. In general, a longer pulse would result in a larger pore. For example, though a longer pulse would provide a much longer-lived driving force for poration, the gradual pore-wetting and start of water-driven flows through the membrane would effectively reduce the transmembrane potential. This would be akin to the drop in voltage across a "leaky/conductive capacitor". So in short, while more pores can conceivably form in areas that might not otherwise be porated by shorter pulses, and existing pores would expand and become larger with longer pulses; the effects may not necessarily scale. Besides, there are possibilities for pores to coalesce. Thus, for example, while a 20 ns pulse may create twice the porated area as a 10 ns pulse, a 600 ns pulse would likely not create 60-times larger effect as compared to the 10 ns pulse.

The physics behind the delay in pore closure can be understood and explained on the basis of the following. The process of applying an external electric field sets into motion two distinct effects. First, the electrical driving force acting on the lipids and dipolar molecules causes a structural re-arrangement of the bilayer and opens up nano-channels [61]. However, this molecular rearrangement in itself is insufficient to attract water molecules from the surrounding aqueous medium into the membrane region. Given the small radii of nanopores formed upon the application of a nanosecond electric pulse and that the hydrophobic interaction prevents water throughput in smaller pores. This is more so for nanopores formed during the ultrashort pulsing than for the larger pores formed with conventional microsecond electroporation. Mere membrane reorganization cannot necessarily support cellular flows. However, if the electric field were applied long enough to facilitate electro-wetting and lowering of the local surface tension, then water molecules could penetrate through the lipid membrane. Thus, the second effect of pulsing is to drive electro-wetting and force water into the nano-channels. Based on classical electrochemistry [62], it is well known that a local electric field can lower the interfacial tension γ according to: $\gamma = \gamma_1 - CV^2 / 2$, where γ_1 is the reference "wettability" in the absence of any electric field, C is the interfacial capacitance, and V the potential difference set up between the liquid and the lipid surface. The process of electro-wetting can alternatively be viewed as an outcome of a Maxwell stress at the boundary of water entering a nanopore.

The affinity of water towards the membrane upon the application of an external electric field is linked to the behavior of the polar water molecules. For liquid water, orientations of water molecules are subject to angle restrictions associated with hydrogen bonding and a strong tendency to minimize the loss of hydrogen bonds at the interface [63,64]. The hydrogen bonding between water molecules favors near-parallel dipole orientations relative to the pore surface upon electric field application. In other words, in order to optimize hydrogen bonding, angular distributions of water molecules relative to the pore walls would be biased against orientations in which the hydrogen atoms point toward the circular walls. As a result of this field-induced dipole re-orientation, the pore could be made to switch from a hydrophobic "off-state" to a hydrophilic "on-state". The hydrophobicity switching should be very fast since it involves the re-orientation of water dipoles as the first step. This is in agreement with the short pore formation times as revealed by the present MD simulations.

The above can also help explain the observed long life of nanopores, and their relative stability over the t = 10 ns to the t = 60 ns duration. Physically, this result would imply that once the water penetrates a nanopore, it does not spontaneously (or quickly) evaporate. Thus, the nanopore does not switch back into a hydrophobic state as soon as the external electric field is turned off. This can alternatively be understood from the standpoint of water repulsion energetics [65]. As shown by Lueng et al. [65], the capillary evaporation activation barrier for a very short 1.4 nm thick layer of water is ~18.7 k_BT for water-hydrocarbon potential, and that evaporation should proceed within a nanosecond time scale. However, a water layer twice as thick (or more) will remain metastable over a long time. Since the membrane thicknesses of a water filled nanopore here are typically on the order of ~5 nm, long-lived nanopores are naturally implied. Incidentally, our result of a long-lived nanopore is in keeping with recent experimental studies by Pakhomov et al. [66] using 600 ns pulses that have shown the nanopores to be stable for many minutes.

It is also perhaps be germane to qualitatively examine if the alignment of water molecules along the channels may have any effects on the transport of ions and molecules. Basically, as is well known, ions in bulk water form hydration layers that make the ion behave as a 'quasi-particle' that includes the ion and tightly bound water molecules. The formation of hydration layers around ions has been known for some time [67], and is due to the strong local electric field around the ion and to repulsive short-range interactions among molecular/atomic species. This quasi-particle is then solvated in the high-dielectric water and oscillations in water density are established with a strong peak about 3 Å away from the ion, and two other oscillations after that spaced about 2 Å apart. As the ion goes from the bulk solution to the pore, it has to partially shed its hydration layers, i.e., the quasi-particle has to break apart. This gives a nonlinearity in the energetic barrier to transport. However, when an ion is placed within a nanopore, the hydration layers would be affected leading to wavelike features that are due to the interference patterns between oscillations reflecting off the walls of the pore (that set an effective pore radius) and those around the ion. These patterns depend on pore size—different pore sizes can give maxima and minima in the water density along the pore axis [68]. Thus basically, the polarization and formation of an ordered dipolar structure around an ion prevent easy passage and require energy to transport the hydrated species. If, however, the water molecules were prevented (or restricted) from freely surrounding the ions, conduction through a pore would increase. In the present case, the hydrogen bonding between water molecules would favor near-parallel dipole orientations relative to the pore surface upon electric field application. This would have the effect of reducing the free availability of water dipoles to "cloak or dress" the ions. The screening (i.e., permittivity) would be reduced, as would be the resistance to ionic flow. Hence, the conductivity would be expected to increase. The reduced permittivity (i.e., screening ability) can alternatively be viewed as a lowering of the Born energy barrier [69] that would contribute to enhanced flow through pores.

Finally, for completeness, we briefly touch upon the important aspect of heating that would likely be associated with multiple pulsing at the high electric fields, though a detailed analysis is beyond the present scope. For example, Croce et al. [70] have numerically calculated the temperature increase across a cell membrane due to pulsed electric fields using a finite element approach. Even a very modest change in temperature of about 1.5 K across a 5 nm thick membrane (and in its immediate vicinity) can lead to an extremely large temperature gradient of about 3×10^8 K/m. Bresme et al. [71] have recently explored the behavior of water under thermal gradients using non-equilibrium Molecular Dynamics simulations. Their report finds that the water molecules tend to adopt a preferred orientation, with the dipole aligning with the temperature gradient and the hydrogen atoms pointing preferentially towards the cold region. The inherent physics is very similar to the thermoelectric effect. It hinges on the relatively faster movement of lighter particles from amongst a collection within a dissimilar group, when energy is gained from a hotter source. Microscopically, in the case of water, the hydrogen bonds are more flexible and hydrogen tends to move over relatively larger distances from the hotter source

as compared to the oxygen ions. Thus in other words, a temperature gradient can re-orient the polar liquid and lead to the build-up of significant local electric fields. In the calculations of Bresme et al. [71], a thermal gradient of 10^7 K/m was shown to produce a local electric field of roughly 10^5 V/m. In the present case of nanosecond, high electric field pulsing, extremely high temperature gradients on the order of 3×10^8 K/m are possible (as discussed above), and so could well lead to local electric fields on the order of 30 kV/cm. Since thermal processes typically have much longer time-scales in comparison to electrical responses, the thermal gradients can be expected to remain well beyond the nanosecond pulsing times. The local electric fields then would be sufficient to enlarge pores and facilitate long-lived transport through the cell membranes subject to such multiple, high intensity pulsing. This aspect has not been examined to our knowledge, and merits detailed study from the standpoint of employing multiple pulse-trains and optimizing their bio-effects. It could also help explain some of the long-lived membrane transport in actual experiments. Also for completeness, it may be mentioned that one would expect the typical thermalization times for the water molecules to be on the order of seconds [72]. Though the thermal gradient magnitudes would slowly decrease over time, these would certainly remain over times much longer than the nanosecond time scales.

5. Conclusions

In summary, we have probed the dynamical translocation of lipids from one leaflet to another due to membrane permeabilization driven by nanosecond, high-intensity (>100 kV/cm) electrical pulses. Most reports on electroporation have tended to focus primarily on the pore creation process. Our simulations show that lipid molecules can translocate by diffusion via the water-filled nanopores which form following structural rearrangement driven by the external electric field. We do make a distinction between such structural re-arrangement and water entry which is a manifestation of electro-wetting. Specifically, here we have probed the pore dynamics over fairly long time scales and studied the response to multiple pulsing. Such simulations over longer times would be relevant to gauge the time duration over which nanopores might remain open, and thus facilitate continued lipid translocations. The two-pulse scenario also enables the study of possible cumulative effects on cell response and membrane transport.

Our results do show that nanopores once formed can remain open for long times. The pore effects would thus likely be much stronger with multiple pulsing. Our microscopic results are indicative of a $N^{½}$ scaling with pulse number for the pore radius, and in keeping with a prediction previously made on the basis of statistical arguments [56]. These results bode well for the use of pulse trains in biomedical engineering applications, not only due to cumulative behaviors, but also due to the possibility of long-lived thermo-electric physics, and the potential for pore coalescence. Finally, as a caveat, it may be added that our results apply in situations where short nanosecond pulses are used, and focus more on the inherent biophysics rather than making direct comparisons with actual biological experiments.

Disclosure

The authors report no conflicts of interest in this study.

Acknowledgements

We would like to thank A. Garner (Purdue University) and D. P. Tieleman (Univ. Calgary) for useful discussions. Partial support from Old Dominion University is gratefully acknowledged. Finally, we like to acknowledge the Texas Advanced Computing Center and Center for Computational Biology and Bioinformatics for resources in carrying out the MD simulations on multiple processors.

References

[1] For example. D. Voet, J.G. Voet, Biochemistry, third ed. John Wiley & Sons, New York, 2004.
[2] R.B. Gennis, Biomembranes: Molecular Structure and Function, Springer-Verlag, New York, 1989.
[3] A. Zachowski, Phospholipids in animal eukaryotic membranes: transverse asymmetry and movement, Biochem. J. 294 (1993) 1–14.
[4] K. Balasubramanian, A.J. Schroit, Aminophospholipid asymmetry: a matter of life and death, Annu. Rev. Physiol. 65 (2003) 701–734.
[5] V.A. Fadok, D.R. Voelker, P.A. Campbell, J.J. Cohen, D.L. Bratton, P.M. Henson, Exposure of phosphatidylserine on the surface of apoptotic lymphocytes triggers specific recognition and removal by macrophages, J. Immunol. 148 (1992) 2207–2216.
[6] S. Manno, Y. Takakuwa, N. Mohandas, Identification of a functional role for lipid asymmetry in biological membranes: phosphatidylserine-skeletal protein interactions modulate membrane stability, Proc. Natl. Acad. Sci. U. S. A. 99 (2002) 1943–1948.
[7] T. Pomorski, S. Hrafnsdottir, P.F. Devaux, G. van Meer, Lipid distribution and transport across cellular membranes, Semin. Cell Dev. Biol. 12 (2001) 139–148.
[8] J. Liu, J.C. Conboy, 1,2-Diacyl-phosphatidylcholine flip-flop measured directly by sum-frequency vibrational spectroscopy, Biophys. J. 89 (2005) 2522–2532.
[9] E.M. Bevers, P. Comfurius, D.W.C. Dekkers, R.F.A. Zwaal, Lipid translocation across the plasma membrane of mammalian cells, Biochim. Biophys. Acta 1439 (1999) 317–330.
[10] T. Pomorski, A.K. Menon, Lipid flippases and their biological functions, Cell. Mol. Life Sci. 63 (2006) 2908–2921.
[11] B. Alberts, D. Bray, J. Lewis, M. Raff, K. Roberts, J.D. Watson, Molecular Biology of the Cell, Garland, New York, 1994.
[12] O.P. Hamill, B. Martinac, Molecular basis of mechanotransduction in living cells, Physiol. Rev. 81 (2001) 685–740.
[13] M. Okino, H. Mohri, Effects of a high-voltage electrical impulse and an anticancer drug on in vivo growing tumors, Jpn. J. Cancer Res. 78 (1987) 1319–1321.
[14] S. Orlowski, J. Behradek Jr., C. Paoletti, L.M. Mir, Transient electropermeabilization of cells in culture. Increase in the cytotoxicity of anticancer drugs, Biochem. Pharmacol. 37 (1988) 4724–4733.
[15] E. Neumann, M. Schaefer-Ridder, Y. Wang, P.H. Hofschneider, Gene transfer into mouse lyoma cells by electroporation in high electric fields, EMBO J. 1 (1982) 841–845.
[16] A.V. Titomirov, S. Sukharev, E. Kistanova, In vivo electroporation and stable transformation ofskin cells of new- born mice by plasmid DNA, Biochim. Biophys. Acta 1088 (1991) 131–134.
[17] U. Zimmermann, Electric field-mediated fusion and related electrical phenomena, Biochim. Biophys. Acta 694 (1982) 227–277.
[18] L.M. Mir, M. Belehradek, C. Domenge, S. Orlowski, J. Poddevin Jr., G. Schwab, B. Luboinnski, C. Paoletti, Electrochemotherapy, a new antitumor treatment: first clinical trial, C.R. Acad. Sci., Ser. III 313 (1991) 613–619.
[19] S. Mehier-Humbert, R.H. Guy, Physical methods for gene transfer: improving the kinetics of gene delivery into cells, Adv. Drug Deliv. Rev. 57 (2005) 733–753.
[20] T. Kodama, Y. Tomita, K.I. Koshiyama, M.J.K. Blomley, Transfection effect of microbubbles on cells in superposed ultrasound waves and behavior of cavitation bubble, Ultrasound Med. Biol. 32 (2006) 905–914.
[21] H. Schneckenburger, A. Hendinger, R. Sailer, W.S.L. Strauss, M. Schmitt, Laser-assisted optoporation of single cells, J. Biomed. Opt. 7 (2002) 410–416.
[22] Y. Shirahata, N. Ohkohchi, H. Itagak, S. Satomi, New technique for gene transfection using laser irradiation, Invest. Med. 49 (2001) 184–190.
[23] S.K. Mohanty, M. Sharma, P.K. Gupta, Laser-assisted microinjection into targeted animal cells, Biotechnol. Lett. 25 (2003) 895–899.
[24] U.K. Tirlapur, K. Koenig, Targeted transfection by femtosecond laser, Nature 418 (2002) 290–291.
[25] I. Vlassiouk, A. Krasnoslobodtsev, S. Smirnov, M. Germann, "Direct" detection and separation of DNA using nanoporous alumina filters, Langmuir 20 (2004) 9913–9915.
[26] F. Rios, S. Smirnov, Nanofluidic ionic diodes: comparison of analytical and numerical solutions, ACS Appl. Mater. Interfaces 1 (2009) 768–774.
[27] D. Wandera, S.R. Wickramasinghe, S.M. Husson, Stimuli-responsive membranes, J. Membr. Sci. 357 (2010) 6–35.
[28] L. Ying, P. Wang, E.T. Kang, K.G. Neoh, Synthesis and characterization of poly(acrylic acid)-graft-poly(vinylidene fluoride) copolymers and pH-sensitive membranes, Macromolecules 35 (2002) 673–679.
[29] R. Casasus, E. Climent, M.D. Marcos, R. Martinez-Martinez, F. Sanceno, J. Soto, P. Amoros, J. Cano, E.J. Ruiz, Dual aperture control on pH- and anion-driven supramolecular nanoscopic hybrid gate-like ensembles, J. Am. Chem. Soc. 130 (2008) 1903.
[30] T.D. Nguyen, K.C.F. Leung, M. Liong, C.D. Pentecost, J.F. Stoddart, J.I. Zink, Construction of a pH-driven supramolecular nanovalve, Org. Lett. 8 (2006) 3363–3366.
[31] J.H. Jang, I. In, Poly(*N*-isopropylacrylamide)-grafted thermosensitive anodized aluminum oxide membrane, Chem. Lett. 39 (2010) 1190–1191.
[32] R.J.C. Gilbert, Pore-forming toxins, Cell. Mol. Life Sci. 59 (2002) 832–844.
[33] Y. Toyoshima, T.E. Thompson, Chloride flux in bilayer membranes: the electrically silent chloride flux in semispherical bilayers, Biochemistry 14 (1975) 1525–1531.
[34] S. Schwarz, C.W.M. Haest, B. Deuticke, Extensive electroporation abolishes experimentally induced shape transformations of erythrocytes: a consequence of phospholipids symmetrization? Biochim. Biophys. Acta 1421 (1999) 361–379.
[35] Q. Hu, R.P. Joshi, K.H. Schoenbach, Simulations of nanopore formation and phos-phatidylserine externalization in lipid membranes subjected to high-intensity, ultrashort electric pulse, Phys. Rev. E 72 (2005) 031902(1-8).

[36] P.T. Vernier, M.J. Ziegler, Y. Sun, W.V. Chang, M.A. Gundersen, D.P. Tieleman, Nanopore formation and phosphatidylserine externalization in a phospholipid bilayer at high transmembrane potential, J. Am. Chem. Soc. 128 (2006) 6288–6289.
[37] R.P. Joshi, K.H. Schoenbach, Bioelectric effects of intense ultrashort pulses, Crit. Rev. Biomed. Eng. 38 (2010) 255–304.
[38] K.H. Schoenbach, R.P. Joshi, J. Kolb, N. Chen, M. Stacey, P. Blackmore, E.S. Buescher, S.J. Beebe, Ultrashort electrical pulses open a new gateway into biological cells, Proc. IEEE 92 (2004) 1122–1137.
[39] S.J. Beebe, P.F. Blackmore, J. White, R.P. Joshi, K.H. Schoenbach, Nanosecond pulsed electric fields modulate cell function through intracellular signal transduction mechanisms, Physiol. Meas. 25 (2004) 1077–1093.
[40] P.T. Vernier, Y. Sun, L. Marcu, S. Salemi, C.M. Craft, M.A. Gundersen, Calcium bursts induced by nanosecond electric pulses, Biochem. Biophys. Res. Commun. 310 (2003) 286–295.
[41] R. Nuccitelli, U. Pliquett, X. Chen, W. Ford, R.J. Swanson, S.J. Beebe, J.F. Kolb, K.H. Schoenbach, Nanosecond pulsed electric fields cause melanomas to self-destruct, Biochem. Biophys. Res. Commun. 343 (2006) 351–360.
[42] S.J. Beebe, N.M. Sain, W. Ren, Induction of cell death mechanisms and apoptosis by nanosecond pulsed electric fields (nsPEFs), Cell 2 (2013) 136–162.
[43] R.P. Joshi, A. Mishra, J. Song, A.G. Pakhomov, K.H. Schoenbach, Simulation studies of ultrashort, high-intensity electric pulse induced action potential block in whole-animal nerves, IEEE Trans. Biomed. Eng. 55 (2008) 1391–1398.
[44] K.H. Schoenbach, B. Hargrave, R.P. Joshi, J.F. Kolb, R. Nuccitelli, C. Osgood, A.G. Pakhomov, M. Stacey, R.J. Swanson, J. White, S. Xiao, J. Zhang, S.J. Beebe, P.F. Blackmore, E.S. Buescher, Bioelectric effects of nanosecond pulses, IEEE Trans. Dielectr. Electr. Insul. 14 (2007) 1088–1109.
[45] H.J.C. Berendsen, D. van der Spoel, R. van Drunen, GROMACS: a message-passing parallel molecular dynamics implementation, Comput. Phys. Commun. 95 (1995) 43–56.
[46] O. Berger, O. Edholm, F. Jahnig, Molecular dynamics simulations of a fluid bilayer of dipalmitoylphosphatidylcholine at full hydration, constant pressure, and constant temperature, Biophys. J. 72 (1997) 2002–2013.
[47] H.J.C. Berendsen, J.P.M. Postma, W.F. van Gunsteren, A. DiNola, J.R. Haak, Molecular dynamics with coupling to an external bath, J. Chem. Phys. 81 (1984) 3684–3690.
[48] T. Darden, D. York, L. Pedersen, Particle mesh Ewald: an $N\cdot\log(N)$ method for Ewald sums in large systems, J. Chem. Phys. 98 (1993) 10089–10092.
[49] B. Hess, H. Bekker, H.J. Berendsen, LINCS: a linear constraint solver for molecular simulations, J. Comput. Chem. 18 (1997) 1463–1472.
[50] E. Lindahl, B. Hess, D. van der Spoel, GROMACS 3.0: a package for molecular simulation and trajectory analysis, J. Mol. Model. 7 (2001) 306–317.
[51] B.L. Ibey, D.G. Mixon, J.A. Payne, A. Bowman, K. Sickendick, G.J. Wilmink, W.P. Roach, A.G. Pakhomov, Plasma membrane permeabilization by trains of ultrashort electric pulses, Bioelectrochemistry 79 (2010) 114–121.
[52] R.E. Brown, D.C. Bartoletti, G.I. Harrison, T.R. Gamble, J.G. Bliss, K.T. Powell, J.C. Weaver, Multiple-pulse electroporation: uptake of a macromolecule by individual cells of *Saccharomyces cerevisiae*, Bioelectrochem. Bioenerg. 28 (1992) 235–245.
[53] K.H. Schoenbach, R.P. Joshi, S.J. Beebe, C. Baum, A scaling law for membrane permeabilization with nanopulses, IEEE Trans. Dielectr. Electr. Insul. 16 (2009) 1224–1235.
[54] A.G. Pakhomov, J. Kolb, J. White, R.P. Joshi, S. Xiao, K.S. Schoenbach, Long-lasting plasma membrane permeabilization in mammalian cells by nanosecond pulsed electric field, Bioelectromagnetics 28 (2007) 655–663.
[55] W. Frey, J.A. White, R.O. Price, P.F. Blackmore, R.P. Joshi, R. Nuccitelli, S.J. Beebe, K.H. Schoenbach, J.F. Kolb, Transmembrane voltage changes during nanosecond pulsed electric exposure, Biophys. J. 90 (2006) 3608–3615.
[56] Z. Vasilkoski, A.T. Esser, T.R. Gowrishankar, J.C. Weaver, Membrane electroporation: the absolute rate equation and nanosecond time scale pore creation, Phys. Rev. E 74 (2006) 021904(1-12).
[57] J.C. Neu, W. Krassowska, Asymptotic model of electroporation, Phys. Rev. E 59 (1999) 3471–3482.
[58] J.C. Weaver, Electroporation of biological membranes from multicellular to nano scales, IEEE Trans. Dielectr. Electr. Insul. 10 (2003) 754–768.
[59] E. Neumann, S. Kakorin, K. Toensig, Fundamentals of electroporative delivery of drugs and genes, Bioelectrochem. Bioenerg. 48 (1999) 3–16.
[60] R. Benz, U. Zimmermann, Pulse-length dependence of the electrical breakdown in lipid bilayer membranes, Biochim. Biophys. Acta 597 (1980) 637–642.
[61] Q. Hu, Z. Zhang, H. Qiu, M.G. Kong, R.P. Joshi, Physics of nanoporation and water entry driven by a high-intensity, ultrashort electrical pulse in the presence of membrane hydrophobic interactions, Phys. Rev. E 87 (2013) 032704(1-9).
[62] E. Dujardin, T.W. Ebbesen, H. Hiura, K. Tanigaki, Capillarity and wetting of carbon nanotubes, Science 265 (1994) 1850–1852.
[63] Q. Du, R. Superfine, E. Freysz, Y.R. Shen, Vibrational spectroscopy of water at the vapor water interface, Phys. Rev. Lett. 70 (1993) 2313–2316.
[64] A. Luzar, S. Svetina, B. Zeks, Consideration of the spontaneous polarization of water at the solid/liquid interface, J. Chem. Phys. 82 (1985) 5146-5144.
[65] K. Leung, A. Luzar, D. Bratko, Dynamics of capillary drying in water, Phys. Rev. Lett. 90 (2003) 065502(1-4).
[66] A.G. Pakhomov, A.M. Bowman, B.L. Ibey, F.M. Andre, O.N. Pakhomova, K.H. Schoenbach, Analysis of conductance of inward-rectifying membrane pores induced by nanosecond electric pulses in GH3 (murine pituitary) and CHO-K1 cells, Biochem. Biophys. Res. Commun. 385 (2009) 181–186.
[67] B. Hille, Ion Channels of Excitable Membranes, Sinauer Associates Inc., Sunderland, MA, 2001.
[68] M. Zwolak, J. Lagerqvist, M.D. Ventra, Quantized ionic conductance in nanopores, Phys. Rev. Lett. (2009) 128102(1-4).
[69] V.A. Parsegian, Ion–membrane interactions as structural forces, Ann. N. Y. Acad. Sci. 264 (1975) 161–174.
[70] R.P. Croce, A. De Vita, V. Pierro, I.M. Pinto, A thermal model for pulsed EM field exposure effects in cells at nonthermal levels, IEEE Trans. Plasma Sci. 38 (2010) 149–155.
[71] F. Bresme, A. Lervik, D. Bedeaux, S. Kjelstrup, Water polarization under thermal gradients, Phys. Rev. Lett. 101 (2008) 020602(1-4).
[72] For example. R.H. Matsunaga, I. dos Santos, Measurement of the Thermal Relaxation Time in Agar-Gelled Water, Conf. Proc. Of the 34th Annual International Conference of the IEEE Engineering in Medicine and Biology Society, San Diego, CA, USA, 28 August–1 September 2012, 2012, pp. 5722–5725.